Optical Materials 58 (2016) 310–316

Contents lists available at ScienceDirect

Optical Materials

journal homepage: www.elsevier.com/locate/optmat

Phase control of six-wave mixing from circularly polarized light

Yunzhe Zhang [a, b], Zhe Liu [b], Hang Wang [a], Shuoke Li [a], Weitao Zhang [b], Wenhui Yi [a], Yanpeng Zhang [a, *]

[a] *Key Laboratory for Physical Electronics and Devices of the Ministry of Education & Shaanxi Key Lab of Information Photonic Technique, Xi'an Jiaotong University, Xi'an 710049, China*

[b] *Institute of Applied Physics, Xi'an University, 710065, China*

A R T I C L E I N F O

Article history:
Received 29 March 2016
Received in revised form
23 May 2016
Accepted 26 May 2016
Available online 7 June 2016

Keywords:
Six-wave mixing
Electromagnetically induced transparency
Circular polarization

A B S T R A C T

We investigate the phase control of six-wave mixing (SWM) in atomic system with multi-Zeeman levels theoretically and experimentally. With the relative phase varying, the switch between bright and dark state can appear in probe transmission signal. Then we demonstrate the evolution of six-wave mixing generated in bright and dark states by scanning the frequency detuning of the dressing field at different polarized probe field. Meanwhile, by utilizing the strong dressing effect of circular polarized light, we observe pure dark state switched to pure bright state in terms of energy level splitting, and compare different phases under different detuning of circularly polarized light. Theoretical calculations are in well agreement with the experimental observations.

1. Introduction

Electromagnetically induced transparency (EIT) [1–3], caused by the quantum coherence and interference, can significantly enhance nonlinear optical properties of the atomic medium [4,5]. Apart from the field of atomic systems, EIT has also been demonstrated an analog in plasmonics, that is, EIT-like or Plasmon-induced transparency (PIT) [6,7]. Recently, some interesting phenomena for Four-wave mixing (FWM) and Six-wave mixing (SWM) in the atomic system were discovered. FWM is used in fiber for generating new lasers in optical communications [8–10], and scientists discovered that FWM can cause the energy transfer of different waves with the self-stabilizing function [11,12]. In addition, SWM as a fifth-order nonlinear effect can be efficiently generated in EIT windows [13–16]. Particularly, the switch between EIT (dark state) and electromagnetically induced absorption (EIA, bright state) [17] has been observed by changing the angle between the probe field and coupling field. Moreover, the switch between dark state (suppression) and bright state (enhancement) in SWM process has been demonstrated by changing the frequency detuning [18,19] and power of light fields [20,21]. However, the phase control in SWM from circularly polarized field is not investigated yet.

In addition, as two or more laser beams pass through an atomic medium, the cross-phase modulation (XPM), as well as modified self-phase modulation (SPM), can potentially affect the propagation and spatial patterns of the propagating laser beams. Self-focusing [22] and pattern formation of laser beam [23] have been extensively investigated with two laser beams propagating in atomic vapors.

In this paper, we study the control mechanism of circularly polarized dressing SWM by the phase of light both experimentally and theoretically. Firstly, we investigate the variation of phase evolution of SWM by changing the polarization of probe field. Then we consider the phase-modulated SWM under circularly polarized probe field. Moreover, we also investigate the spatial images of probe transmission signals (PTS) and SWM signals. Finally, the SWM under different probe field detuning is given out.

2. Theoretical model and experimental scheme

In an inverted-Y type energy level system (with Zeeman sublevels), as shown in Fig. 1 (a) and (d), four laser beams with same diameter of about 1 mm are applied to the atomic system with the spatial configuration given in Fig. 1(b) and (c). The atom density is about $1.0 \times 10^{12}\text{cm}^{-3}$ and the 10 cm long rubidium cell is wrapped by μ-metal and heated by the heater tape. The energy level

* Corresponding author.
E-mail address: 123470592@qq.com (Y. Zhang).

http://dx.doi.org/10.1016/j.optmat.2016.05.052
0925-3467/

configuration is constructed by four energy levels $[|0\rangle 5S_{1/2}(F=3),\ |1\rangle 5P_{3/2}(F=3),\ |2\rangle 5D_{5/2}(F=2),\ |3\rangle 5S_{1/2}(F=2)]$. The probe laser beam $\boldsymbol{E}_1$ (wavelength of 780.24 nm, connecting the transition $|0\rangle 5S_{1/2}(F=3)$ to $|1\rangle 5P_{3/2}(F=3)$) with horizontal polarization is from an external cavity diode laser (ECDL). The laser beam $\boldsymbol{E}_2$ (wavelength of 775.98 nm, connecting transition $|1\rangle 5P_{3/2}(F=3)$ to $|2\rangle 5D_{5/2}(F=2)$) with vertical polarization is from the second ECDL. The third ECDL produces the beams $\boldsymbol{E}_3$ and $\boldsymbol{E}_3'$ (wavelength of 780.24 nm, connecting the transition $|1\rangle 5P_{3/2}(F=3)$ to $|3\rangle 5S_{1/2}(F=2)$) with the horizontal polarization.

In normal spatial configuration, the laser beams are aligned in a square-box pattern as shown in Fig. 1(b). A weak probe field $\boldsymbol{E}_1$ (frequency ω_1, wave vector $\boldsymbol{k}_1$, and Rabi frequency G_1) is modulated by a quarter-wave plate (QWP). Here, we define the frequency detuning as $\Delta_i = \Omega_i - \omega_i$, where Ω_i is the resonance frequency. Two coupling fields $\boldsymbol{E}_3$ (ω_3, k_3, and G_3) and $\boldsymbol{E}_3'$ (ω_3, k_3', and G_3') propagate in the opposite direction of the beam $\boldsymbol{E}_1$ with a small angle ($\sim 0.3^\circ$) between them. Next, we add a strong dressing beam $\boldsymbol{E}_2$ (ω_2, k_2 and G_2), which propagates in the opposite direction of $\boldsymbol{E}_1$. $G_i = \mu_i \boldsymbol{E}_i/\hbar$ is the Rabi frequency with transition dipole moment μ_i. Further, the configuration is modified by introducing an extra small angle φ_2 between $\boldsymbol{E}_2$ and the opposite direction of $\boldsymbol{E}_1$, as shown in Fig. 1(c). With the configuration, a SWM signal with phase matching condition $\boldsymbol{k}_s = \boldsymbol{k}_1 + \boldsymbol{k}_2 + \boldsymbol{k}_3 - \boldsymbol{k}_3' + \boldsymbol{k}_2 - \boldsymbol{k}_2$ is generated by the beams $\boldsymbol{E}_1$, $\boldsymbol{E}_2$, $\boldsymbol{E}_3$ and $\boldsymbol{E}_3'$, and the SWM signals will fall into the $|0\rangle - |1\rangle - |2\rangle$ ladder-type EIT window. Meanwhile, the probe transmission signals (PTS) and SWM signals can be split by polarizing beam splitter (PBS), the images of S-polarized PTS and SWM signals are captured by a charge coupled device (CCD) camera, and the P-polarized spectrum signals are recorded by two avalanche photo diodes (APDs).

In our experimental system, the polarization of probe field $\boldsymbol{E}_1$ is changed by the rotation angle of one QWP as shown in Fig. 1(c), so the probe field $\boldsymbol{E}_1$ can be decomposed into linearly and circularly polarized components, while other beams keep linearly polarized. In this experiment, we make P-polarization direction as the quantization direction and the S-polarized component is decomposed into balanced left- and right-circularly polarized parts. Fig. 1(d) depicts Zeeman transition channels among $5S_{1/2}(F=2,\ 3)$, $5P_{3/2}(F=3)$, $|1\rangle 5P_{3/2}(F=3)$ and $5D_{5/2}$ $(F=2)$ sublevels. There exist many transitions among Zeeman sublevel to generate different SWM signals. Different transition paths associate with Clebsch-Gordan (CG) coefficients [24] can determine the intensities of SWM signals, because it makes the dipole moment μ_{ij} as well as G_i change. The dotted lines, dot-dashed lines, and dashed lines and long dashed lines represent the linear P-polarized, left hand circularly polarized, and right hand circularly polarized $\boldsymbol{E}_1$ field, respectively. Also, the long dashed lines are the linear P-polarized $\boldsymbol{E}_3$ fields, while the double-arrow thin lines are the linear P-polarized fields $\boldsymbol{E}_2$.

From Fig. 1(d), when $\boldsymbol{E}_1$ is linearly P-polarized, according to the perturbation chain $|0_{(M)}\rangle \xrightarrow{G_1^0} |1_{(M)}\rangle$ and $|0_{(M)}\rangle \xrightarrow{G_1^0} |1_{(M)}\rangle_{G_1^0 G_i^{00}\pm} \xrightarrow{(G_3'^{00})^*} |3_{(M)}\rangle \xrightarrow{G_3^{00}} |1_{(M)}\rangle_{G_1^0 G_i^{00}\pm} \xrightarrow{G_2^{00}} |2_{(M)}\rangle \xrightarrow{(G_2^{00})^*} |1_{(M)}\rangle_{G_1^0 G_i^{00}\pm}$ ($i = 2$, 3, 4 and M $= \pm 2, \pm 1$), the first-order density-matrix element $\rho_{10}^{(1)}$ (related with PTS) and the fifth-order density-matrix element $\rho_{S_M}^{(5)0}$ (related with SWM) are written as:

$$\rho_{10}^{(1)} = \sum\nolimits_{M=-2}^{2} iG_{1_M}^{0(\pm)} \Big/ \left[m_1 + \left(G_{3_M}^{00(\pm)} \right)^2 \Big/ \left(\Gamma_{3_M 0_M} + i(\Delta_1 - \Delta_3) \right) \right] \quad (1)$$

$$\rho_{S_M}^{(5)0} = \sum_M \frac{iG_{1_M}^{0} |G_{3_M}|^2 |G_{2_M}|^2}{m_1^3 \left(\Gamma_{3_M 0_M} + i(\Delta_1 - \Delta_3) \right) \left(\Gamma_{2_M 0_M} + i(\Delta_1 + \Delta_2) \right)} \quad (2)$$

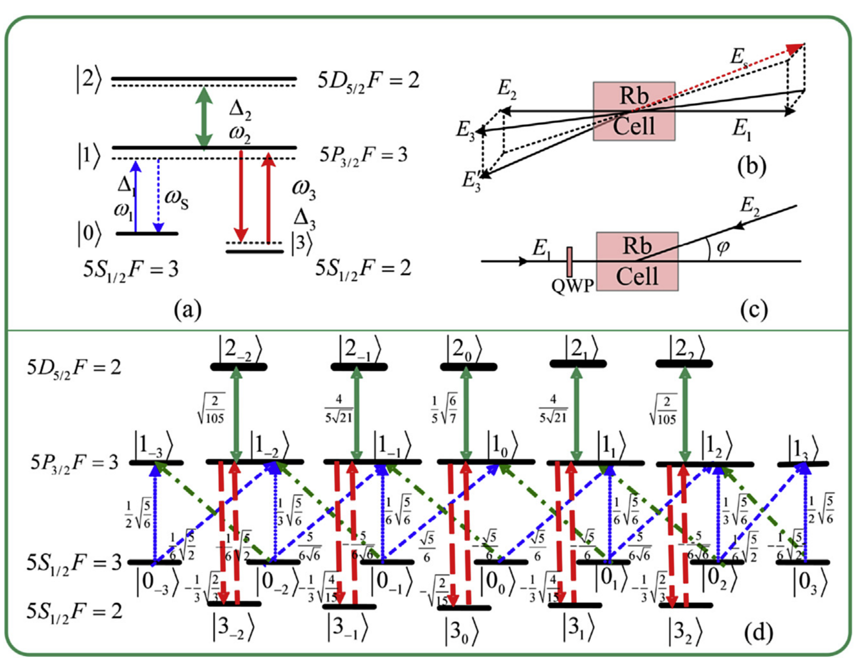

Fig. 1. (a) Four-level atomic system used in experiment. (b) Phase-matching configuration with $\boldsymbol{E}_2$ propagating in the opposite direction of $\boldsymbol{E}_1$. (c) Abnormal configuration where $\boldsymbol{E}_1$ and $\boldsymbol{E}_2$ intersect with a small phase φ_2. (d) The corresponding Zeeman sublevels with various transition pathways. Double-arrow thin lines: dressing field $\boldsymbol{E}_2$; linearly (dot lines), left (dot-dash lines) circularly and right (dash lines) circularly polarized probe fields; long-dash lines: the coupling fields $\boldsymbol{E}_3$ and $\boldsymbol{E}_3'$.